

Fission fragment angular momentum in ODD-Z fissioning systems

H. Naik, S.P. Dange, R.J. Singh

Radiochemistry Division, Bhabha Atomic Research Centre, Trombay, Mumbai-400 085, India

Received: 26 March 1999 / Revised version: 16 October 1999

Communicated by J. Äystö

Abstract. Independent isomeric yield ratios of ^{128}Sb , ^{130}Sb , ^{132}Sb , ^{131}Te , ^{133}Te , ^{132}I , ^{134}I , ^{136}I , ^{135}Xe and ^{138}Cs have been determined in the fast neutron induced fission of ^{237}Np and ^{241}Am using radiochemical and gamma spectrometric technique. From the independent isomeric yield ratios, fragment angular momenta (J_{rms}) have been deduced using spin-dependent statistical model analysis. Comparison of these data with the literature data for even-Z fissioning systems shows the following important features: (i) Angular momenta for fragments with spherical 82n shell and even-Z products are lower compared to the fragments with out the 82n shell and odd-Z products indicating the effect of nuclear structure. (ii) Angular momentum of even-Z products in all the fissioning systems are comparable where as for odd-Z products it is slightly higher in the odd-Z fissioning systems than in the adjacent even-Z fissioning systems. This indicates the role of single particle on fragment angular momentum in odd-Z fissioning systems.

1 Introduction

In low energy fission of actinides, fragment angular momentum arises due to statistical population of various collective modes such as wriggling, bending and twisting [1,2] besides the contribution from the post-scission Coulombic torque [2–4] and/or the single particle excitation. Studies on the fragment angular momentum thus provide an insight into the influence of rotational degrees of freedom at the point of scission and just after the scission. Fragment angular momentum is estimated from physical methods based on measurements of anisotropy [3,4] and multiplicity of the prompt gamma rays [5,6]. These methods generally provide mass averaged angular momenta. The physical method based on the population of the ground-state rotational bands of even-even fission products [7] involving statistical model analysis has been used to estimate the corresponding fragment angular momenta. The angular momenta of even-even fission products have also been determined recently [8] using γ - γ - γ coincidence method with the availability of crystal balls and gamma spheres built from sophisticated high resolution Compton suppressed Ge detectors. On the other hand, determination of independent isomeric yield ratios of both even and odd-Z fission products followed by statistical model analysis has been used for estimating the fragment angular momenta [9–24]. In this method the independent isomeric yield ratios of the fission products are determined using physical techniques based on recoil mass separator [9–11], isotope

separator, ISOL [12] or by radiochemical method [13–24] depending upon the half-lives of the radionuclides. The physical technique based on recoil mass separator [9–11] provides the fragment angular momentum of the fission product as a function of fragment kinetic (excitation) energy where as in the radiochemical method it is possible to obtain the angular momentum of fission products at the average kinetic (excitation) energy. These studies show that fragment angular momentum depends upon nuclear structure effect [15–24] such as odd-even effect [15–20], shell closure proximity [17–24], quadrupole moment [7], scission point deformation [19–21] and fragment kinetic (excitation) energy [8–11]. An inverse correlation of fragment angular momentum with elemental yield was also observed due to coupling between the collective and intrinsic degrees of freedom [19–21]. The observed trend of decreasing angular momentum with increasing kinetic energy [9–11] for different fragments also confirm this fact besides the effect of fragment deformation. However, all these observations are based on the data in the even-Z fissioning systems from Th-Cf except the data of ^{133}Xe and ^{135}Xe in $^{242}\text{Am}^m$ (n_{th},f) [23]. Thus it seems that the data in the odd-Z fissioning systems are extremely rare. In the present work the fragment angular momenta of ^{128}Sb , ^{130}Sb , ^{132}Sb , ^{131}Te , ^{133}Te , ^{132}I , ^{134}I , ^{136}I , ^{135}Xe and ^{138}Cs have been deduced from the radiochemically determined independent isomeric yield ratios in the fast neutron induced fission of ^{237}Np and ^{241}Am . These data are compared with the data of even-Z fissioning systems

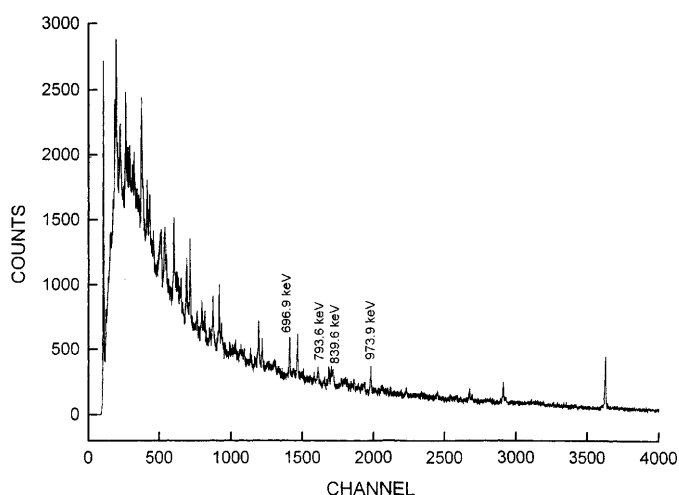


Fig. 1. Direct gamma ray spectrum of fission products from the fast neutron induced fission of ^{241}Am

to examine the single particle effect of odd-Z fissioning system on fragment angular momentum. The effect of nuclear structure on fragment angular momentum has also been discussed.

2 Experimental and calculations

Nitrate solutions of ^{237}Np ($\sim 75 \mu\text{g}$) and ^{241}Am ($\sim 50 \mu\text{g}$) sealed in polypropylene tubes and covered with 1 mm thick cadmium foil were irradiated for 3 min to 5 min at a flux $5 \times 10^{12} \text{ n cm}^{-2} \text{ s}^{-1}$ using the pneumatic carrier facility of reactor CIRUS. Similarly electrodeposited targets of ^{237}Np ($\sim 150 \mu\text{g}$) and ^{241}Am ($\sim 100 \mu\text{g}$) covered with 0.0025 cm thick superpure aluminium catcher foil and wrapped with 1 mm thick cadmium foil were irradiated for 20 min to 60 min at a flux $1.2 \times 10^{12} \text{ n cm}^{-2} \text{ s}^{-1}$ in the reactor APSARA. The irradiated solutions or catcher foils were either for direct gamma ray spectrometry to make measurements on antimony and xenon isotopes whereas they were used for radiochemical separations [25] of tellurium [17,19], iodine [18,21] and caesium [15,16]. Standard aliquots of the separated samples or the irradiated solution or the aluminium catcher were analysed gamma ray spectrometrically using a precalibrated 80 cm^3 HPGe detector coupled to a PC based 4K channel analyser. The resolution of the detector system was 2.0 keV at 1332.0 keV and the dead time was always less than 10%. A typical direct gamma ray spectrum from the 3 min irradiated solution of ^{241}Am is shown in Fig. 1. From Fig. 1 the gamma lines of fission products such as ^{130}Sb and ^{132}Sb are clearly observed inspite of the gamma lines of ^{241}Am . The gamma lines of ^{135}Xe were observed in the gamma ray spectrum of 15–20 min cooled sample. On the other hand the gamma lines of ^{128}Sb were observed from the gamma ray spectrum of 20–60 min irradiated sample. However the gamma lines of $^{131,133}\text{Te}$, $^{132,134}\text{I}$ and ^{138}Cs were not very clear from the direct gamma ray spectrum. For this purpose tellurium, iodine and caesium were separated radiochemically [15–19,25]. A typical gamma ray spectrum

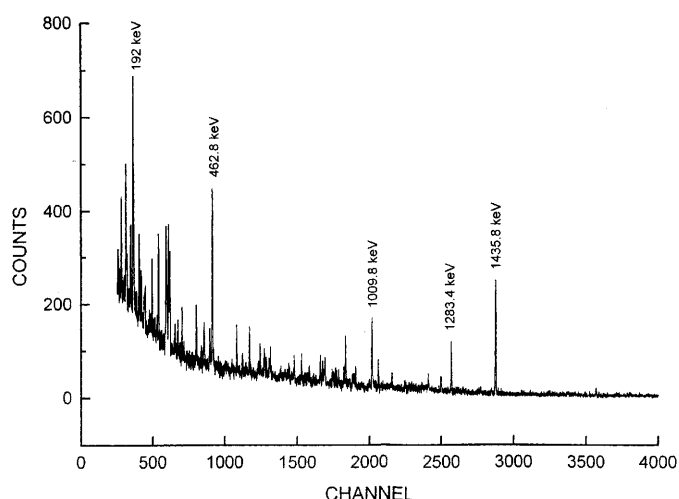


Fig. 2. Gamma ray spectrum of radiochemically separated Cs from the fast neutron induced fission of ^{241}Am

of radiochemically separated Cs from irradiated solution of ^{241}Am is shown in Fig. 2. The gamma lines of ^{138}Cs which otherwise were not visible in the gamma ray spectrum of unseparated sample is very clear from Fig. 2. From the photopeak areas of the gamma rays of the nuclides of interest, independent isomeric yields were determined using usual decay-growth equations [15–24] after correcting for the precursor contribution. The nuclear spectroscopic data of different nuclides in the present work were taken from [20,26,27]. The cumulative yields of the precursors were either determined in the present work or taken from literature [28–32]. The activities of ^{92}Sr , ^{104}Tc in the unseparated samples and ^{134}Te , ^{135}I and ^{139}Cs in the separated samples of tellurium, iodine and caesium were used as fission rate monitors.

3 Results and discussion

The independent isomeric yield ratios of ^{128}Sb , ^{130}Sb , ^{132}Sb , ^{131}Te , ^{133}Te , ^{132}I , ^{134}I , ^{136}I , ^{136}Xe and ^{138}Cs in the fast neutron induced fission of ^{237}Np and ^{241}Am determined in the present work are given in the Table 1. The uncertainty on the isomeric yield ratios include the errors due to the counting statistics, absolute abundance of the gamma lines, detector efficiencies, the fission yields of the precursor and the least square analysis. From the independent isomeric yield ratios, fragment angular momenta (J_{rms}) were deduced using spin dependent statistical model analysis [33] as reported earlier [20,21] and they are given in the same Table 1. With the exception of the data of ^{133}Xe and ^{135}Xe in $^{242}\text{Am}^m(n_{th},f)$ [23] the present set of data determined in the fast neutron induced fission of ^{237}Np and ^{241}Am are being reported for the first time in the odd-Z fissioning systems. The independent isomeric yield ratio of ^{135}Xe from the present work in $^{241}\text{Am}(n,f)$ is seen to be in agreement with the data of Ford et al. [23] in $^{242}\text{Am}^m(n_{th},f)$ though the angular momentum values are different. This is most probably due to the different

Table 1. Independent isomeric yield ratio, fragment J_{rms} and different parameters related to scission-point configuration in the fast neutron induced fission of ^{237}Np and ^{241}Am

Nuclide	IY (%)	$Y_h/(Y_h + Y_l)$	J_{rms}	β	C	T	K.E. (MeV)	
	$(Y_h + Y_l)^a$						(\hbar)	(fm)
$^{238}\text{Np}^*$								
^{128}Sb	0.610 ± 0.086	0.518 ± 0.080	10.2 ± 1.3	0.73	1.05	0.75	176.0	176.9
^{130}Sb	1.414 ± 0.250	0.470 ± 0.157	0.5 ± 1.9	0.59	1.06	0.73	178.0	178.6
^{132}Sb	1.432 ± 0.186	0.377 ± 0.085	7.5 ± 1.0	0.17	1.07	0.68	181.0	180.3
^{131}Te	1.576 ± 0.214	0.653 ± 0.056	5.5 ± 0.4	0.13	1.06	0.69	178.0	178.2
^{133}Te	3.743 ± 0.135	0.570 ± 0.027	4.7 ± 0.3	0.001	1.12	0.62	180.0	188.3
^{132}I	0.540 ± 0.024	0.486 ± 0.047	8.0 ± 0.7	0.70	1.08	0.71	181.0	181.1
^{134}I	2.817 ± 0.248	0.429 ± 0.071	8.2 ± 1.1	0.31	1.07	0.68	179.5	179.4
^{136}I	2.561 ± 0.338	0.684 ± 0.105	8.4 ± 1.5	0.33	1.06	0.68	178.5	177.7
^{135}Xe	0.401 ± 0.073	0.613 ± 0.130	5.0 ± 1.5	0.011	1.07	0.64	179.0	180.5
^{138}Cs	1.238 ± 0.038	0.703 ± 0.084	9.8 ± 1.5	0.62	1.06	0.70	176.0	176.4
$^{242}\text{Am}^*$								
^{128}Sb	0.175 ± 0.029	0.575 ± 0.166	11.1 ± 2.4	0.93	1.07	0.75	185.0	184.9
^{130}Sb	0.844 ± 0.182	0.506 ± 0.137	10.0 ± 2.0	0.73	1.08	0.72	186.0	186.6
^{132}Sb	1.519 ± 0.120	0.385 ± 0.072	7.6 ± 0.9	0.19	1.08	0.67	187.0	186.6
^{131}Sb	1.446 ± 0.108	0.694 ± 0.078	5.9 ± 0.7	0.27	1.08	0.68	186.5	186.3
^{133}Te	3.378 ± 0.316	0.583 ± 0.037	4.9 ± 0.5	0.011	1.08	0.65	186.5	186.3
^{132}I	0.323 ± 0.043	0.526 ± 0.038	9.5 ± 0.5	0.64	1.09	0.70	187.0	187.6
^{134}I	2.458 ± 0.228	0.465 ± 0.047	8.7 ± 0.5	0.44	1.08	0.68	185.7	185.9
^{136}I	1.618 ± 0.187	0.743 ± 0.113	9.7 ± 2.1	0.63	1.07	0.70	184.0	184.2
^{135}Xe	1.728 ± 0.217	0.622 ± 0.138	5.4 ± 1.6	0.12	1.08	0.66	185.0	185.4
^{138}Cs	1.053 ± 0.087	0.719 ± 0.088	10.2 ± 1.9	0.71	1.06	0.70	182.0	181.4

^a Y_h and Y_l = Yield of high and low spin isomers.

code used by them [23] to deduced the fragment angular momentum. The present data are compared with the data [20] of even-Z fissioning systems (i.e. $^{230}\text{Th}^*$ to $^{250}\text{Cf}^*$ and $^{252}\text{Cf}(\text{SF})$) and are discussed below from different point of view.

3.1 Effect of nuclear structure on fragment angular momentum

The fragment angular momentum (J_{rms}) values from Table 1 in the fast neutron induced fission of ^{237}Np and ^{241}Am as a function of the atomic number of the fragment are shown in Fig. 3. Figure 4 shows the fragment J_{rms} of various isotopes of different elements such as antimony, tellurium, iodine and xenon from present work in $^{238}\text{Np}^*$ and $^{242}\text{Am}^*$ and for other fissioning systems from literature [20,23] as a function of fissionability parameter. In Fig. 3 the J_{rms} of various fission fragments in $^{238}\text{Np}^*$ and $^{242}\text{Am}^*$ are shown with their limits of error whereas in Fig. 4 the limits of error are not shown. This is because the J_{rms} of so many fission fragments in large number of fissioning systems starting from $^{230}\text{Th}^*$ to $^{250}\text{Cf}^*$ and $^{252}\text{Cf}(\text{SF})$ have been included for comparison. Thus showing the limits of error in Fig. 4 will make the figure clumsy.

It can be seen from Fig. 3 that odd-Z fragments have higher angular momentum than the neighboring even-Z ones [15–20]. This indicates the odd-even effect on fragment angular momentum. The higher angular momen-

tum of odd-Z fragments is due to single particle effect or due to higher deformation of the odd-Z fragment resulting from the polarization of the even core by an odd proton as indicated by Madsen and Brown [34]. On the other hand from Fig. 4 it can be seen that, the fragment angular momenta of ^{132}Sb , ^{133}Te , ^{134}I and ^{135}Xe are lower than $^{128,130}\text{Sb}$, $^{131,132}\text{Te}$, $^{132,136}\text{I}$ and $^{133,138}\text{Xe}$ respectively. From the point view of bending mode oscillation model [2] it is expected that heavy mass fragment should have higher angular momentum than light mass fragment. The contradictory observation of lower angular momentum of ^{132}Sb , ^{133}Te , ^{134}I and ^{135}Xe compared to other fission products is due to the presence of spherical 82n shell in their fragment stage since the number of neutron emitted in the mass range 132–136 is around one. This indicates the effect of shell closure proximity. A similar effect of shell configuration is evident from the higher fragment J_{rms} of fission products having deformed 66n, 88n shell in their fragment stage [7,8,19–21]. These observations indicate that fragment angular momentum depend on their deformation at scission. The effect of deformation is further observed from the higher fragment J_{rms} for the fission products in the rare earth region having permanent ground state deformation [7,14,19–21]. Recent observation of higher angular momentum because of super deformation for $^{144,146}\text{Ba}$ and ^{104}Mo in $^{252}\text{Cf}(\text{S.F.})$ [8] from γ - γ - γ coincidence measurements confirms this fact. Further, the decrease of fragment angular momentum with increase in kinetic energy for various fission products in the thermal

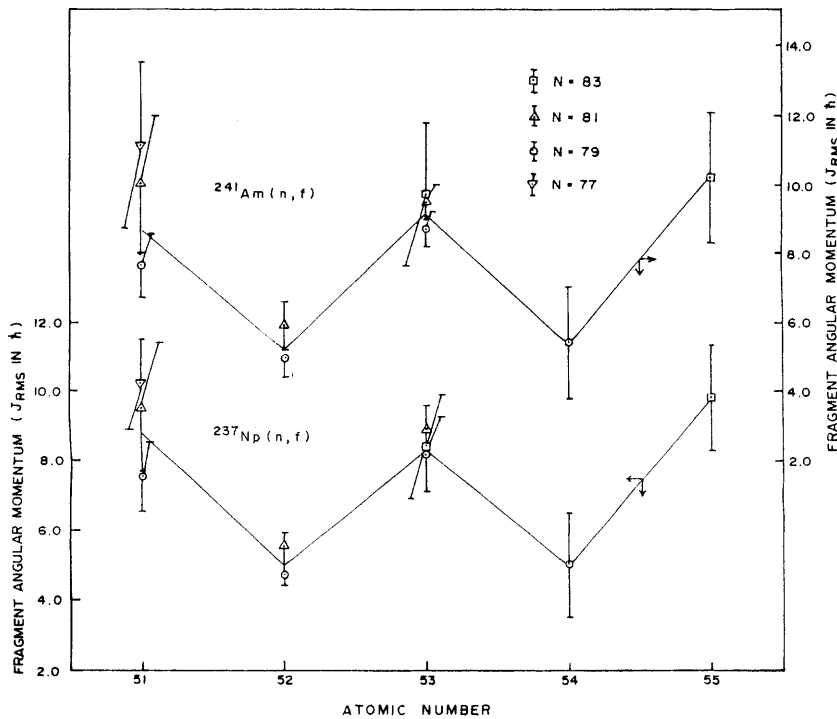


Fig. 3. The plot of fragment angular momentum (J_{rms}) as a function of atomic number of fission product in the fast neutron induced fission of ^{237}Np and ^{241}Am

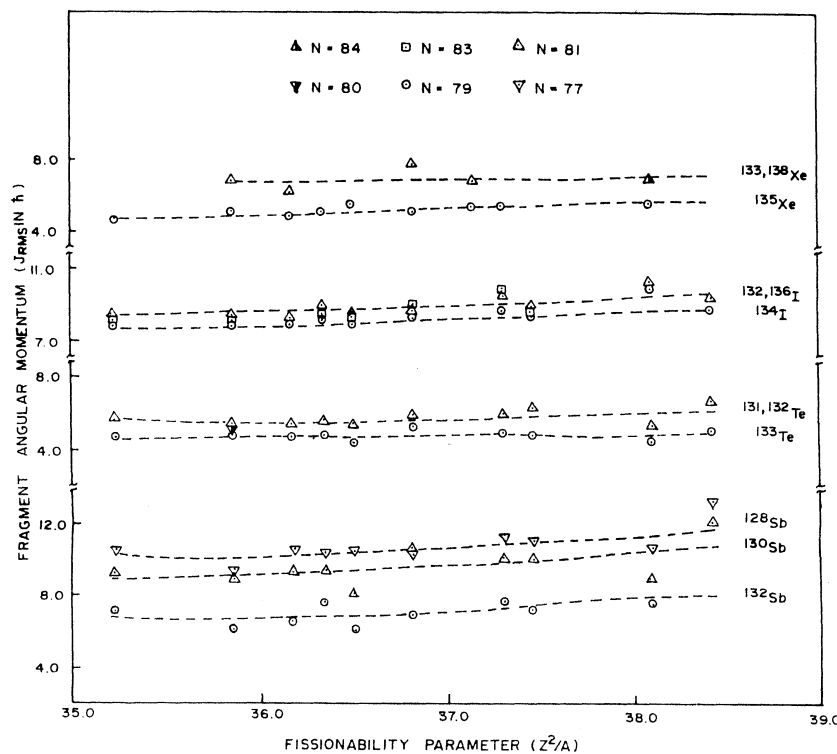


Fig. 4. The plot of fragment angular momentum (J_{rms}) as a function of fissionability parameter (Z_F^2/A_F)

neutron induced fission of $^{233,235}\text{U}$ and ^{239}Pu from the recoil mass separated data [9-11] also support the above fact. However Wilhelmy et al. [7] mentioned that there is no correlation between fragment angular momentum and scission point deformation. This observation is based on the plot of fragment angular momentum of only even-even fission products vs. average neutron number in $^{252}\text{Cf}(\text{S.F.})$

where they did not see any correlation. On the other hand Bocquet et al. [9] have indicated that in $^{235}\text{U}(n_{th}, f)$ the fragment angular momentum deduced from the prompt gamma rays and the theoretical values calculated by Dietrich shows a saw tooth nature similar to that of the average neutron number as a function of fission product mass. This observation supports the correlation of frag-

ment angular momentum with the scission point deformation. Other than these observations it can also be seen from Fig. 4 that the fragment angular momentum of even-Z products (^{131}Te , ^{133}Te , ^{133}Xe and ^{135}Xe) are more or less comparable in both even and odd-Z fissioning systems. However, the angular momentum of odd-Z products in odd-Z fissioning systems ($^{238}\text{Np}^*$ and $^{242}\text{Am}^*$) are slightly higher than in the neighboring even-Z fissioning systems ($^{234,236}\text{U}^*$, $^{240,242}\text{Pu}^*$ and $^{246}\text{Cm}^*$) [20]. Even if one considers the error limits (not shown in Fig. 4) then also the observation remains unaltered. This is because the component of errors are common to all the data points and the relative error is somewhat smaller. Thus the above observation is most probably due to the fact that odd-Z fragments in odd-Z fissioning systems are more deformed at the cost of their even-Z complementary fragments. Besides this, the extra single particle spin in odd-Z fissioning systems might contribute to the odd-Z fragments resulting in higher angular momentum. These observations clearly show that the fragment angular momenta are related on the one hand to their nuclear structure effect through deformation at the scission and on the other to single particle effect. In order to examine these aspects the fragment deformation at the scission point were evaluated from the fragment angular momentum as described earlier [19–21] by us in the case of even-Z fissioning systems.

3.2 Calculation of scission point deformation

Deformation parameter (β) for different fragments at the scission in the fast neutron induced fission of ^{237}Np and ^{241}Am were calculated as prescribed by Datta et al. [19] on the basis of the origin of angular momentum from the pre-scission bending mode [2] and statistical considerations [1,7]. Assuming statistical equilibrium among the various collective degrees [1,7], the RMS angular momentum (J_{rms}) of the fragment is given as [7]

$$J_{rms}^2 = 2IT/\hbar^2 \quad (1)$$

where I is the temperature (T) and deformation (β) dependent moment of inertia given as [24]

$$I = I_{rig}[1 - 0.8 \exp(-0.693E^*/5)] \quad (2)$$

E^* is the excitation energy of the fragment given by

$$E^* = aT^2, \quad a = A/8 \text{ MeV}^{-1} \quad (3)$$

On the other hand, according to the pre-scission bending oscillation model [2,7] the average angular momentum (J_{av}) of the fragment is given as

$$J_{av} = \sqrt{\pi/2\gamma} - 0.5, \quad J_{av} = \sqrt{\pi/2}J_{rms} \quad (4)$$

where γ is the bending mode oscillation amplitude or the angular positional uncertainty. γ is approximately related [7] to the neck radius (c) and the semi-major axis (z) at deformation (β) as [35]

$$\gamma = c/z, \quad z = R(\beta)[1 + \sqrt{5/4\pi\beta}] \quad (5)$$

where $R(\beta)$ is the radius considering volume conservation given as

$$R(\beta) = R[1 - 15/16\pi\beta^2 + 0.25(5/4\pi)^{3/2}\beta^3]^{-1/3} \quad (6)$$

The neck radius, c , can also be related to the deformation parameter (β) through the scission point distance (D) and thus with the fragment kinetic energy (E_K) on the basis of the condition [19] of equality of the Coulomb and nuclear forces at the scission point as

$$Z(Z_F - Z)e^2/D^2 = 2\pi c^2\Omega/\lambda, \quad D = z_1 + z_2 \quad (7)$$

$$E_K = (1 - A/A_F)E, \quad E = Z(Z_F - Z)e^2/D \quad (8)$$

where Ω and λ are the coefficient and range of the attractive nuclear force, usually taken as 1.107 MeV/fm² and 0.68 fm respectively [36]. A_F and Z_F are the mass and charge of the fissioning nucleus, E is the total kinetic energy.

From the above equations it is seen that the calculation of the deformation parameter (β) for a given fragment from its J_{rms} value requires the knowledge of either T or c for the corresponding split which is not known with any certainty. It was however, shown by Wilkins et al. [37] that fragment deformation (β) (0.95 times the Bohr–Mottelson parameter) varies up to 1.0 for various fragments and T might be 1.0 MeV. On the other hand Wilhelmy et al. [7] showed that the c -value to be in the range of 1.0 to 1.6 fm. In view of these considerations, the J_{rms} for each fragment was calculated within 1 \hbar of the experimental value using both the statistical correlation and bending oscillation model by varying β from 0.001 to 1.0, the T value from 0.3 to 2.0 MeV and the c -value from 0.5 to 2.0 fm respectively. Thus the c - and T -values resulting in the approximate fragment J_{rms} for each β -value were deduced. Subsequently for each value of c , the kinetic energy (E) for that particular split was calculated using (7) and (8). The appropriate values of β , T and c for a fragment were then sorted out comparing the calculated kinetic energy with the experimental one [38–41]. Since the kinetic energy for an individual split (i.e. as a function of charge for fixed mass) is not known, the experimental kinetic energy [38–41] for a particular mass corresponding to the average charge was used. The calculated deformation parameter (β), temperature (T), neck radius (c) and kinetic energy (E) along with experimental values are given in Table 1. In the case of odd-Z fragments the observed J_{rms} is likely to be influenced by the odd particle spin of the fragment itself. For such fragments, β -values were calculated after correcting the fragment J_{rms} for the single particle spin ($2\hbar$) effect. The possible contribution due to post-scission Coulombic torque was not considered as this contribution was evaluated [2–7] to be low, within 1–2 \hbar (the same as the uncertainty on the experimental J_{rms} values) and since, it does not enhance fragment spin consistently [2,7]. Besides these, the probable contribution of the single particle spin from the odd-Z fissioning system to the spin of the fragment was not considered.

It can be seen from Table 1 that, the β -values for the fragments having spherical 82n shell and even-Z products are lower than that for the fragments with out 82n

shell and odd-Z products as expected similar to the even-Z fissioning systems [20]. The β -values for the fragments having 82n shell are seen to be in agreement with the theoretical estimates of Wilkins et al. [37]. The β -values of different fragments in $^{237}\text{Np}(n,f)$ and $^{241}\text{Am}(n,f)$ from the present work are compared with the same in even-Z fissioning systems ($^{230}\text{Th}^*$, $^{234,236}\text{U}^*$, $^{240,242}\text{Pu}^*$, $^{246}\text{Cm}^*$, $^{250}\text{Cf}^*$ and $^{252}\text{Cf}(\text{SF})$) from our earlier work [20]. It is observed that the β -value of even-Z fragments are more or less comparable in both even and odd-Z fissioning systems. However the β -values of odd-Z fragments are higher in odd-Z fissioning systems ($^{238}\text{Np}^*$ and $^{242}\text{Am}^*$) than in their neighboring even-Z fissioning systems ($^{234,236}\text{U}^*$, $^{240,242}\text{Pu}^*$ and $^{246}\text{Cm}^*$). This is most probably due to the fact that, odd-Z fragments in odd-Z fissioning systems are more deformed at the cost of their even-Z complementary fragments.

In conclusion it can be said that:

- (i) The fragment angular momentum depends on nuclear structure effects such as shell-closure proximity and odd-even effect.
- (ii) Angular momentum of even-Z products are comparable in all the fissioning systems, whereas for odd-Z products it is slightly higher in the odd-Z fissioning systems than in the even ones. This is due to the single particle spin contribution from odd-Z fissioning system to the odd-Z fragments or due to the higher deformation of the odd-Z fragments at the cost of their even-Z complementary fragments.
- (iii) Fragment scission-point deformations deduced from fission fragments angular momenta are seen to be in good agreement with the theoretical value obtained from the static scission point model.

The authors wish to express their sincere thanks to Dr. S.B. Manohar, Head Radiochemistry Division for his keen interest and encouragement in this work. Thanks are also due to Dr. R.H. Iyer emeritus scientist (CSIR) for his valuable suggestions.

References

1. Nix, J.R., Swiatecki, W.J.: Nucl. Phys. **71**, 1 (1965)
2. Rasmussen, J.O., Norenberg, W., Mang, H.J.: Nucl. Phys. **A136**, 465 (1969)
3. Hoffman, M.M.: Phys. Rev. **133**, B714 (1964)
4. Strutinski, V.M.: So. Phys. JETP **10**, 613 (1960)
5. Nifenecker, H., Signarbieux, C., Ribrag, M., Poitou, J., Matuszek, J.: Nucl. Phys. **A189**, 285 (1972)
6. Armbruster, P., Labus, H., Reichelt, K.: Naturforsch. **A269**, 512 (1971); Plesonton, F., Ferguson, R.L., Schmitt, H.W.: Phys. Rev. **C6**, 1023 (1972)
7. Wilhelmy, J.B., Cheifetz, E., Jared, R.C., Thompson, S.G., Bowman, H.R., Rasmussen, J.R.: Phys. Rev. **C5**, 2041 (1972)
8. Ter-Akopian, G.M., Hamilton, J.H., Oganessian, Yu.Ts., Danniell, A.V., Kormicki, J., Ramayya, A.V., Popeko, G.S., Babu, B.R.S., Lu, Q.-H., Butler-Moore, K., Ma, W.-C., Jones, E.F., Deng, J.K., Shi, D., Kliman, J., Morhac, M., Cole, J.D., Aryaeinejad, R., Johnson, N.R., Lee, I.Y., McGowan, F.K.: Phys. Rev. **C55**, 1146 (1997)
9. Bocquet, J.P., Schussler, F., Monnard, E., Sistemich, K.: Proc. Fourth IAEA Symp. on Physics and Chemistry of fission, Julich, Vol. II, p. 179. IAEA, Vienna, 1979
10. Denschlag, H.O., Braun, H., Faubel, W., Fischbach, G., Meixler, H., Paffarth, G., Porsch, W., Weis, M., Schrader, H., Siegert, G., Blachot, J., Alfassi, Z.B., Erten, H.N., Izakbiran, T., Tamai, T., Wahl, A.C., Wolfsberg, K.: Proc. Fourth IAEA Symp. on Physics and Chemistry of fission, Julich Vol. II, p. 153. IAEA, Vienna, 1979
11. Denschlag, H.O.: Proc. Symp. on Radiochemistry and Radiation Chemistry IGCAR, Kalpakkam, India p. IT-10 (1989)
12. Rudstam, G., Aagaard, P., Ekstrom, B., Lund, E., Gokturk, H., Zwicky, H.U.: Radiochim. Acta **49**, 155 (1990)
13. Sarantities, D.G., Gordon, G.E., Coryell, C.D.: Phys. Rev. **138**, B353 (1965)
14. Aumann, D.C., Guckel, W., Nirschl, E., Zeising, H.: Phys. Rev. **C16**, 254 (1977)
15. Fujiwara, I., Imanishi, N., Nishi, T.: Phys. Soc. Jpn. **51**, 1713 (1982)
16. Tomar, B.S., Goswami, A., Das, S.K., Datta, T., Prakash, S., Ramaniah, M.V.: Radiochim. Acta **39**, 1 (1985)
17. Dange, S.P., Naik, H., Data, T., Guin, R., Prakash, S., Ramaniah, M.V.: J. Radioanal. Nucl. Chem. Lett. **108**, 269 (1986)
18. Dange, S.P., Naik, H., Datta, T., Reddy, A.V.R., Prakash, S., Ramaniah, M.V.: Radiochim. Acta **39**, 127 (1986)
19. Datta, T., Dange, S.P., Das, S.K., Prakash, S., Ramaniah, M.V.: Z. Phys. **A324**, 81 (1986)
20. Naik, H., Dange, S.P., Singh, R.J., Datta, T.: Nucl. Phys. **A587**, 273 (1995)
21. Naik, H., Datta, T., Dange, S.P., Pujari, P.K., Prakash, S., Ramaniah, M.V.: Z. Phys. **A331**, 335 (1988)
22. Tomar, B.S., Goswami, A., Reddy, A.V.R., Das, S.K., Manohar, S.B., Prakash, S.: Radiochim. Acta **55**, 173 (1991)
23. Ford, G.P., Wolfsberg, K., Erdal, B.R.: Phys. Rev. **C30**, 195 (1984)
24. Imanishi, N., Fujiwara, I., Nishi, T.: Nucl. Phys. **A263**, 141 (1976)
25. Flynn, K.: Argonne National Laboratory Report ANL 75-25 (1975)
26. Browne, E., Firestone, R.B.: Table of radioactive isotopes, ed. Shirley, V.S. (Wiley, New York, 1986)
27. Blachot, J., Fiche, Ch.: Table of radioactive isotopes and their main decay characteristics, Ann. Phys. **6**, 3-218 (1981)
28. Iyer, R.H., Naik, H., Pandey, A.K., Kalsi, P.C., Singh, R.J., Ramaswami, A., Nair, A.G.C.: Nucl. Sci. Eng. (cmuicated).
29. Stella, R., Moretto, L.G., Maxia, V., Casa, Di., Respi, V., Rollier, M.A.: J. Inorg. Nucl. Chem. **31**, 3739 (1969)
30. Ramaswami, A., Rattan, S.S., Chakravarty, N., Singh, R.J., Manohar, S.B., Prakash, S., Ramaniah, M.V.: Radiochim. Acta **41**, 9 (1987)
31. Reddy, A.V.R.: Ph. D. Thesis, Sri Venkateswara University, Tirupati, India (1986)
32. Rickard, R.R., Goecking, C.F., Wyatt, I.: Nucl. Eng. **23**, 115 (1965)
33. Huizenga, J.R., Vandenbosch, R.: Phys. Rev. **120**, 1305 (1960); Hafner, W.L., Huizenga, J.R., Vandenbosch, R.: Argonne National Laboratory Report ANL-6662 (1962)

34. Madsen, V.A., Brown, V.R.: Phys. Rev. Lett. **52**, 176 (1984); Madsen, V.A., Brown, V.R., Anderson, J.D.: Phys. Rev. **C12**, 1205 (1975)
35. Shultheis, H., Schultheis, R.: Phys. Rev. **C18**, 317 (1978)
36. Davies, K.T.R., Sierk, A.J., Nix, J.R.: Phys. Rev. **C13**, 2385 (1976)
37. Wilkins, B.D., Steinberg, E.P., Chasman, R.R.: Phys. Rev. **C14**, 1832 (1976)
38. Bennett, M.J., Stein, W.E.: Phys. Rev. **156**, 1277 (1967)
39. Dange, S.P., Ramaswami, A., Manohar, S.B., Prakash, S., Ramaniah, M.V.: Phys. Rev. **C11**, 1251 (1977)
40. Prakash, S., Manohar, S.B., Dange, S.P., Ramaswami, A., Ramaniah, M.V.: Radiochim Acta. **18**, 35 (1972)
41. Asghar, M., Caitukoli, F., Perrin, P., Barreau, G., Guet, C.R., Leroux, B., Signarbieux, C.: Proc. IAEA Symposium on Physics and Chemistry of fission, Julich, Vol. II, p. 81. IAEA, Vienna, 1980